

**Transient analytical solution for one-dimensional transport of organic contaminants through GM/GCL/SL composite liner**

Shi-Jin Feng<sup>a,\*</sup>, Ming-Qing Peng<sup>a</sup>, Zhang-Long Chen<sup>a</sup>, Hong-Xin Chen<sup>a</sup>

<sup>a</sup> Key Laboratory of Geotechnical and Underground Engineering of Ministry of Education, Department of Geotechnical Engineering, Tongji University, Shanghai 200092, China.

\* Corresponding author

Email addresses: fsjgly@tongji.edu.cn (Shi-Jin Feng); pengmq@tongji.edu.cn (Ming-Qing Peng); chenzhanglong@tongji.edu.cn (Zhang-Long Chen); chenhongxin@tongji.edu.cn (Hong-Xin Chen)

**ABSTRACT:** Analytical solution for transport of organic contaminants through composite liner consisting of a geomembrane (GM), a geosynthetic clay liner (GCL), and a soil liner (SL) with finite thickness is presented. The transient diffusion-advection processes in the whole composite liner and adsorption in GCL and SL can be described by the present method. The method is successfully verified against analytical solution to a coupling transient diffusion-advection problem in double-layer porous media. The rationality of the steady-state transport assumption in GM and GCL and the semi-infinite bottom boundary assumption, which are widely adopted in the existing works, is comprehensively investigated. The overestimated zone, underestimated zone and no difference zone caused by the two assumptions under various conditions are identified. With the increase of elapsed time, the overestimated zone disappears, and the underestimated zone becomes smaller and smaller and finally is overwhelmed by the no difference zone. Moreover, the equivalency between GM/GCL/SL and GM/CCL composite liners is also properly assessed by the present method. GM/GCL/SL composite liner performs better than GM/CCL composite liner under high leachate level condition.

**Keywords:** Landfill; Advection; Diffusion; Liner system; Analytical solution.

## 1 Introduction

Municipal Solid Waste (MSW) landfills and hazardous waste landfills are important sources of groundwater pollution (Qiu, 2011; Han et al., 2016; Postigo et al., 2018). Organic contaminants are among the most hazardous constituents in landfill leachate (Kjeldsen et al., 2002), because they are generally toxic at lower concentration than many inorganic compounds (Edil, 2003; Islam and Rowe, 2008). Composite liner, which generally consists of a geomembrane (GM) layer, a compacted clay liner (CCL) or a geosynthetic clay liner (GCL) and a soil liner (SL), has been widely used in landfills to protect surrounding environment and groundwater from landfill leachate pollution (Barroso et al., 2006; Bouazza and Bowder, 2010; Varank et al., 2011a; El-Zein et al., 2012; Park et al., 2012; Hoor and Rowe, 2013; Guan et al., 2014; Xie et al., 2015a). Therefore, it is substantially essential to study the transport of organic contaminants in composite liners.

The prediction of organic contaminant transport through composite liner, however, is quite difficult and intricate for three main reasons. First, composite liner inherently consists of two or even more layers with distinctly different transport properties (Rowe, 2012). Second, the potential mechanisms involved in the transport process are various and complicated, mainly including diffusion, advection and adsorption (Lake and Rowe, 2005; Chen et al., 2015; Xie et al., 2015b). Third, the concentration at a certain point in composite liner changes over time until equilibrium is reached (Foose, 2002; Edil, 2003; El-Zein, 2008). For these reasons, accurately estimating the performance of composite liner system is a challenging work, and great efforts have been made to solve the problem. This study will focus on analytical solutions.

In the past decades, numerous solutions have been proposed for contaminant migration in composite liners (Liu and Ball, 1998; Foose, 2002; Shackelford and Lee, 2005; Chen et al., 2009; Liu et al., 2009; Cleall and Li, 2011; Zhan et al., 2013). However, only diffusion is

considered in these solutions. Extensive literature indicates that apart from diffusion, leakage through the geomembrane defects and the underlying SL should also be considered when assessing the performance of landfill composite liners (El-Zein, 2008; Du et al., 2009; El-Zein et al., 2012; Rowe, 2012; Rowe and Abdelatty, 2013), especially in cases with high frequency of holes and high hydraulic leachate head.

Fortunately, several analytical solutions considering diffusion and advection through single layer porous media (Guerrero and Skaggs, 2010; Varank et al., 2011b; Guerrero et al., 2013; Singh and Das, 2015; Singh et al., 2017), double-layer porous media (Li and Cleall, 2011) and composite liners (Guan et al., 2014; Chen et al., 2015) have been developed. For example, Li and Cleall (2011) presented a transient analytical solution for solute transport in double-layer porous media. Guan et al. (2014) and Chen et al. (2015) presented quasi-steady-state analytical solution for solute transport through composite liner consisting of a GM layer or a GCL overlaying a SL. However, the solutions proposed by Li and Cleall (2011), Guan et al. (2014) and Chen et al. (2015) are only applicable for two-layer liners and cannot be directly applied for composite liners with multiple layers. In fact, composite liner consisting of a GM layer overlaying GCL and SL has been widely used in landfills. However, there is scanty analytical solution available for solute transport through a multilayered composite liner considering the coupling effect of diffusion and advection.

Recently, Xie et al. (2015a) has proposed an analytical solution for diffusion and advection transport through a composite liner consisting of GM, GCL and SL, which is the state-of-the-art for this problem (denoted as Steady-state and Semi-infinite Method (SSM)). However, there are still some limitations. First, steady-state transport in GM and GCL is assumed, namely, it is assumed that the contaminant concentration in GM and GCL do not change over time (denoted as steady-state assumption). In fact, contaminant transport through the whole composite liner is a transient process (Foote, 2002). Second, the bottom boundary

condition cannot be properly modeled since the SL is assumed to be semi-infinite (denoted as semi-infinite assumption). However, the thickness of SL is definitely finite rather than semi-infinite. The above two assumptions highly simplify the problem, but the rationality of the hypotheses is still questionable and the applicable conditions should be thoroughly investigated.

The main purpose of this paper is to develop transient analytical solution for transport of organic contaminants through a GM/GCL/SL composite liner considering finite thickness of SL. A particular focus of this paper is to identify the limitation of the semi-infinite assumption and the steady-state assumption on evaluating the performance of the composite liner. In addition, the equivalence of performance between GM/CCL and GM/GCL/SL composite liners is also analyzed using the proposed solution.

## 2 Mathematical model development

### 2.1 Basic assumptions

As shown in Fig. 1, the liner system is composed of three individual horizontal layers, namely a GM, a GCL and a SL. Advection and diffusion occur in all the three layers, and adsorption of the contaminant occurs in the GCL and SL layers.  $L_{gm}$ ,  $L_{gcl}$  and  $L_{sl}$  represent the thicknesses of the GM, the GCL and the SL, respectively;  $L_{cl}$  is the thickness of the composite liner;  $h_w$  is the hydraulic leachate head mounding on the GM surface. Several assumptions are adopted to facilitate developing the mathematical model: (1) contaminant concentration in the leachate is assumed to be constant at  $C_0$  (Chen et al., 2009); (2) the GCL and the SL are both saturated and homogeneous (Benson et al., 1999; Stark, 2017); (3) contaminant transport is one-dimensional along  $z$  axis (Chen et al., 2015); (4) degradation of the organic contaminants is neglected (Chen et al., 2015); (5) adsorption of the contaminant in GCL and SL is a linear and equilibrium process (Rowe, 1998).

## 2.2 Governing equations and boundary conditions

As the governing equation for GM is not exactly the same as that for GCL and SL, which results in much difficulty in obtaining the solution for the whole composite liner, a normalization method is proposed to deal with the governing equations and boundary conditions for GM. Consequently, a normalized general governing equation that is applicable for all the three layers is finally obtained, which is the key to get the transient solution for the whole composite liner.

### (1) GM layer

The transient transport of contaminants through GM can be described by the following equation:

$$\frac{\partial C_{\text{gm}}(z, t)}{\partial t} = D_{\text{gm}} \frac{\partial^2 C_{\text{gm}}(z, t)}{\partial z^2} - \frac{v_a}{K_g} \frac{\partial C_{\text{gm}}(z, t)}{\partial z} \quad (1)$$

where  $C_{\text{gm}}(z, t)$  is the contaminant concentration in GM at any position  $z$  and any time  $t$ ;  $D_{\text{gm}}$  is the diffusion coefficient of GM;  $K_g$  is the partition coefficient between GM and the landfill leachate, which is the ratio of the contaminant concentration at equilibrium in GM to that in the leachate;  $v_a$  is the Darcy velocity of contaminant in the composite liner. The detailed derivation of the governing equation is given in Appendix A. In fact, the transport model for GM will reduce to a model similar to that in the existing works (Xie et al., 2015a, 2015b, 2015c; Chen et al., 2015) if the contaminant transport in GM is assumed to be a steady-state process.

The top boundary condition at the interface between GM and leachate can be expressed as follows (Leo, 1971; Sangam and Rowe, 2005):

$$C_{\text{gm}}(0, t) = C_0 K_g \quad (2)$$

### (2) GCL layer

The governing equation for the contaminant transport through GCL is

$$\frac{\partial C_{\text{gcl}}(z, t)}{\partial t} = \frac{D_{\text{gcl}}}{R_{\text{d,gcl}}} \frac{\partial^2 C_{\text{gcl}}(z, t)}{\partial z^2} - \frac{v_{\text{gcl}}}{R_{\text{d,gcl}}} \frac{\partial C_{\text{gcl}}(z, t)}{\partial z} \quad (3)$$

where  $C_{\text{gcl}}(z, t)$  is the contaminant concentration in GCL at any position  $z$  and any time  $t$ ;  $D_{\text{gcl}}$  is the effective diffusion coefficient of GCL;  $v_{\text{gcl}}$  is the seepage velocity in GCL;  $R_{\text{d,gcl}}$  is the retardation factor of GCL and can be determined by

$$R_{\text{d,gcl}} = 1 + \frac{\rho_{\text{d,gcl}} K_{\text{d,gcl}}}{n_{\text{gcl}}} \quad (4)$$

where  $\rho_{\text{d,gcl}}$  is the dry density of GCL;  $n_{\text{gcl}}$  is the porosity of GCL and  $K_{\text{d,gcl}}$  is the distribution coefficient of GCL, reflecting the adsorption capacity of the GCL. Similar to GM, the transport model for GCL will reduce to that in the existing works (Guan et al., 2014; Xie et al., 2015a, 2015c; Chen et al., 2015) if the contaminant transport in GCL is assumed to be a steady-state process. In fact, the steady-state assumption in the existing works causes that adsorption cannot be considered in GCL.

The continuity conditions at the interface between GM and GCL can be expressed as

$$\frac{C_{\text{gm}}(L_{\text{gm}}, t)}{K'_g} = C_{\text{gcl}}(L_{\text{gm}}, t) \quad (5)$$

$$v_a \frac{C_{\text{gm}}(L_{\text{gm}}, t)}{K'_g} - D_{\text{gm}} \frac{\partial C_{\text{gm}}(L_{\text{gm}}, t)}{\partial z} = n_{\text{gcl}} v_{\text{gcl}} C_{\text{gcl}}(L_{\text{gm}}, t) - n_{\text{gcl}} D_{\text{gcl}} \frac{\partial C_{\text{gcl}}(L_{\text{gm}}, t)}{\partial z} \quad (6)$$

where  $K'_g$  is the partition coefficient between GM and GCL, which is assumed to be equal to  $K_g$  (Chen et al., 2009).

### (3) SL layer

The governing equation for contaminant transport through SL is (Xie et al., 2015a)

$$\frac{\partial C_{\text{sl}}(z, t)}{\partial t} = \frac{D_{\text{sl}}}{R_{\text{d,sl}}} \frac{\partial^2 C_{\text{sl}}(z, t)}{\partial z^2} - \frac{v_{\text{sl}}}{R_{\text{d,sl}}} \frac{\partial C_{\text{sl}}(z, t)}{\partial z} \quad (7)$$

where  $C_{\text{sl}}(z, t)$  is the contaminant concentration in SL at any position  $z$  and any time  $t$ ;  $D_{\text{sl}}$  is the effective diffusion coefficient of SL;  $v_{\text{sl}}$  is the seepage velocity in SL;  $R_{\text{d,sl}}$  is the retardation

factor of SL and can be determined by

$$R_{d,sl} = 1 + \frac{\rho_{d,sl} K_{d,sl}}{n_{sl}} \quad (8)$$

where  $\rho_{d,sl}$  is the dry density of SL;  $n_{sl}$  is the porosity of SL;  $K_{d,sl}$  is the distribution coefficient of SL, reflecting the adsorption capacity of the SL.

The continuity conditions between GCL and SL can be expressed as

$$C_{gcl}(L_{gm} + L_{gcl}, t) = C_{sl}(L_{gm} + L_{gcl}, t) \quad (9)$$

$$n_{gcl} D_{gcl} \frac{\partial C_{gcl}(L_{gm} + L_{gcl}, t)}{\partial z} = n_{sl} D_{sl} \frac{\partial C_{sl}(L_{gm} + L_{gcl}, t)}{\partial z} \quad (10)$$

The bottom boundary conditions that may exist beneath a composite liner can be expressed as

$$C_{sl}(L_{cl}, t) = 0 \quad (\text{for the Dirichlet boundary}) \quad (11)$$

$$\frac{\partial C_{sl}(L_{cl}, t)}{\partial z} = 0 \quad (\text{for the Neumann boundary}) \quad (12)$$

These bottom boundary conditions are able to properly model contaminant transport through the bottom of a composite liner (Foote, 2002). Eq. (11) represents a leakage detection layer or layer conducting flow that instantaneously removes all the contaminant from the base of the system and Eq. (12) represents an impermeable base stratum (Chen et al., 2009). In comparison, the bottom boundary of SSM is assumed to be semi-infinite even though the thickness of composite liner is finite.

Initially, there is no contaminant in the composite liner. Thus, the initial condition is

$$\begin{bmatrix} C_{gm}(z, 0) \\ C_{gcl}(z, 0) \\ C_{sl}(z, 0) \end{bmatrix} = 0 \quad (13)$$

Darcy velocity in each layer is a significant parameter in terms of contaminant advection through the composite liner. Rowe (1998) has developed a simple equation to predict leakage

rate through a hole in a GM coincident with a wrinkle:

$$Q = \frac{2h_w L_w}{l} (kb + \sqrt{kl\theta}) \quad (14)$$

where  $Q$  is the leakage rate through the composite liner ( $\text{m}^3/\text{s}$ );  $L_w$  is the length of the connected wrinkles (m);  $2b$  is the width of the wrinkle (m);  $l$  is the thickness of the underlying liners (m);  $\theta$  is the transmissivity of the interface between GM and GCL ( $\text{m}^2/\text{s}$ );  $k$  is the hydraulic conductivity of the underlying liners (m/s). Foose et al. (2001) reported that Eq. (14) agrees well with the results of numerical analysis. Thus, the Darcy velocity in the composite liner can then be obtained by (Rowe and Brachman, 2004)

$$v_a = mQ / A \quad (15)$$

where  $m$  is the number of defects in GM per unit area;  $A$  is the cross-sectional area of the flow.

In this case,  $k$  is the harmonic mean of hydraulic conductivities of GCL and SL:

$$k = \frac{L_{\text{gcl}} + L_{\text{sl}}}{L_{\text{gcl}} / k_{\text{gcl}} + L_{\text{sl}} / k_{\text{sl}}} \quad (16)$$

where  $k_{\text{gcl}}$ ,  $k_{\text{sl}}$  are the hydraulic conductivities of GCL and SL, respectively.

Finally, the seepage velocity in GCL and SL can be derived from Darcy velocity by  $v_a = n_{\text{gcl}}v_{\text{gcl}} = n_{\text{sl}}v_{\text{sl}}$ .

(4) Normalized general governing equation

The forms of the governing equations for GCL (Eq. (3)) and SL (Eq. (7)) are the same, but are different from that for GM (Eq. (1)). To facilitate the derivation of the solution, a normalized general governing equation is required, namely, it is demanded that the governing equations for GM, GCL and SL share the same expression.

The contaminant concentration in GM can be normalized by partition coefficient

$$C_{\text{gm}}^*(z, t) = \frac{C_{\text{gm}}(z, t)}{K_g} \quad (17)$$

where  $C_{\text{gm}}^*(z, t)$  is the normalized contaminant concentration in GM at any position  $z$  and any

time  $t$ .

By substituting Eq. (17) into Eq. (2), the top boundary condition can be described by

$$C_{\text{gm}}^*(z=0, t) = C_0 \quad (18)$$

By substituting Eq. (17) into Eq. (5), the continuity condition of concentration between GM and GCL can be described by

$$C_{\text{gm}}^*(z=L_{\text{gm}}, t) = C_{\text{gcl}}(z=L_{\text{gm}}, t) \quad (19)$$

The governing equation for GM (Eq. (1)) can also be rewritten in the form of  $C_{\text{gm}}^*(z, t)$ . Notably, the contaminant mass flux in GM computed by the normalized concentration must be the same as that computed using the actual concentration. As a consequence, the spatial dimension of GM,  $z$  ( $0 \leq z \leq L_{\text{gm}}$ ), must also be normalized by partition coefficient:

$$z^* = z / K_g \quad (0 \leq z^* \leq L_{\text{gm}} / K_g) \quad (20)$$

where  $z^*$  is the normalized spatial dimension for GM, so that the calculated contaminant mass fluxes in GM by the actual parameters and the normalized parameters can be the same:

$$v_a \frac{C_{\text{gm}}(z, t)}{K_g} - D_{\text{gm}} \frac{\partial C_{\text{gm}}(z, t)}{\partial z} = v_a C_{\text{gm}}^*(z^*, t) - D_{\text{gm}} \frac{\partial C_{\text{gm}}^*(z^*, t)}{\partial z^*} \quad (21)$$

Finally, the governing equation for GM (Eq. (1)) can be rewritten in the form of normalized concentration and normalized thickness of GM (i.e.,  $C_{\text{gm}}^*(z^*, t)$ ) as follows:

$$\frac{\partial C_{\text{gm}}^*(z^*, t)}{\partial t} = \frac{D_{\text{gm}}}{K_g^2} \frac{\partial^2 C_{\text{gm}}^*(z^*, t)}{\partial z^{*2}} - \frac{v_a}{K_g^2} \frac{\partial C_{\text{gm}}^*(z^*, t)}{\partial z^*} \quad (22)$$

In addition, by substituting Eq. (20) into Eq. (18), Eqs. (17) and (20) into Eqs. (6) and (19), the top boundary condition and the continuity conditions between GM and GCL, in the form of  $C_{\text{gm}}^*(z^*, t)$  are obtained.

Obviously, by replacing  $n_{\text{gm}}$ ,  $R_{\text{d, gm}}$ ,  $z$  ( $0 \leq z \leq L_{\text{gm}}$ ) and  $C_{\text{gm}}(z, t)$  with 1,  $K_g^2$ ,  $z^*$  ( $0 \leq z^* \leq L_{\text{gm}}/K_g$ ) and  $C_{\text{gm}}^*(z^*, t)$ , respectively, the expressions for contaminant transport through GM

have the same form as those for GCL and SL, including the governing equation and the boundary conditions.

Eventually, contaminant transport through the composite liner system can be simply described by the normalized general governing equation:

$$\frac{\partial C_i(z,t)}{\partial t} = \frac{D_i}{R_{d,i}} \frac{\partial^2 C_i(z,t)}{\partial z^2} - \frac{v_i}{R_{d,i}} \frac{\partial C_i(z,t)}{\partial z}, \quad i=1, 2, 3 \quad (23)$$

where  $i = 1, 2, 3$  represents GM, GCL and SL, respectively. The normalized general continuity conditions at the GM/GCL and the GCL/SL interfaces are

$$C_i(z = L_i, t) = C_{i+1}(z = L_i, t), \quad i = 1, 2 \quad (24)$$

$$n_i D_i \frac{\partial C_i(z = L_i, t)}{\partial z} = n_{i+1} D_{i+1} \frac{\partial C_{i+1}(z = L_i, t)}{\partial z}, \quad i = 1, 2 \quad (25)$$

In addition, the corresponding normalized top and bottom boundary conditions can be obtained from Eqs. (11), (12) and (18). Finally, the origin problem is normalized.

### 2.3 Solution

The normalized problem described by Eqs. (23-25) can be transformed into two sub-problems by submitting Eq. (26) into Eq. (23):

$$C_i(z,t) = u_i(z)C_0 + w_i(z,t), \quad i = 1, 2, 3 \quad (26)$$

The governing equation of the sub-problem 1 can be expressed as

$$\frac{D_i}{R_{d,i}} \frac{d^2 u_i(z)}{dz^2} - \frac{v_i}{R_{d,i}} \frac{du_i(z)}{dz} = 0, \quad i = 1, 2, 3 \quad (27)$$

The general solution to the sub-problem 1 can be readily derived from Eq. (27) as

$$u_i(z) = k_{i,1} e^{r_{i,1}z} + k_{i,2} e^{r_{i,2}z}, \quad i = 1, 2, 3 \quad (28)$$

where  $k_{i,1}$ ,  $k_{i,2}$ ,  $r_{i,1}$  and  $r_{i,2}$  can be obtained using the boundary and continuity conditions (Eqs. (B2-B9)). The detailed derivation of the solution is given in Appendix B.

The governing equation of the sub-problem 2 can be expressed as

$$\frac{\partial w_i(z,t)}{\partial t} = \frac{D_i}{R_{d,i}} \frac{\partial^2 w_i(z,t)}{\partial z^2} - \frac{v_i}{R_{d,i}} \frac{\partial w_i(z,t)}{\partial z}, \quad i=1, 2, 3 \quad (29)$$

The general solution can be derived using separation of variables method from Eq. (29)

as

$$w_i(z,t) = \sum_{m=1}^{\infty} C_m g_{m,i}(z) e^{a_i z - \beta_m t}, \quad i=1, 2, 3 \quad (30)$$

$C_m$ ,  $a_i$  are coefficients;  $\beta_m$  are eigenvalues of the composite liner.

When  $\beta_m - v_i^2/(4D_i R_{d,i}) \geq 0$ ,

$$g_{m,i}(z) = A_{m,i} \sin(\mu_i \lambda_{m,i} z) + B_{m,i} \cos(\mu_i \lambda_{m,i} z); \quad i=1, 2, 3 \quad (31a)$$

When  $\beta_m - v_i^2/(4D_i R_{d,i}) < 0$ ,

$$g_{m,i}(z) = A_{m,i} \sinh(\mu_i \lambda_{m,i} z) + B_{m,i} \cosh(\mu_i \lambda_{m,i} z); \quad i=1, 2, 3 \quad (31b)$$

To determine the coefficients in the solution, the following procedures should be done.

(1) Substituting the solution (Eqs. (30) and (31)) into the governing equation (Eq. (29)),  $a_i$ ,  $\lambda_{m,i}$  and  $\mu_i$  (Eqs. (C.12)-(C.14)) are obtained.

(2) Substituting Eqs. (30) and (31) into the continuity conditions (Eqs. (C.3) and (C.4)), recursive equations of  $A_{m,i}$ ,  $B_{m,i}$  (Eq. (C.15)) and a transfer matrix  $T_i$  (Eq. (C.16)) are obtained.

(3) Substituting Eqs. (30) and (31) into the bottom boundary condition (Eq. (C.7) or Eq. (C.8)), a characteristic equation (Eq. (C.18)) is obtained and the matrix  $T_3$  (Eq. (C.19) or Eq. (C.20)) is given for case considering Dirichlet or Neumann bottom boundary condition.

(4) Substituting Eqs. (30) and (31) into the top boundary condition (Eq. (C.2)), the matrix  $T_0$  (Eq. (C.21)) is obtained.

(5) The coefficient  $C_m$  could be obtained by orthogonality condition (Eq. (C.22)).

(6) Substituting the obtained  $T_3$ ,  $T_0$  and  $T_i$  into the characteristic equation (Eq. (C.18)),  $\beta_m$  are determined. Consequently, all the coefficients in solution for the sub-problem 2 are obtained.

The coefficients in solution for the sub-problem 1 could be determined following the similar procedures. Thus, substituting the solutions for the two sub-problems (Eqs. (28) and (30)) into Eq. (26), the solution for the original problem is finally obtained. The detailed derivation of the solution for the two sub-problems are given in Appendix B and Appendix C, respectively.

### **3 Model verification**

A coupling transient diffusion-advection problem in double-layer porous media reported by Li and Cleall (2011) is chosen to verify the proposed method. The thicknesses of both layers are 0.5 m. The effective diffusion coefficient, the retardation factor and the porosity of the top layer are  $5 \times 10^{-9}$  m<sup>2</sup>/s, 2 mL/g and 0.4, respectively; and those for the bottom layer are  $10 \times 10^{-9}$  m<sup>2</sup>/s, 1 mL/g and 0.6, respectively. The solute concentration at the top boundary is fixed at  $C_0 = 1$  mg/L. The initial solute concentration in the composite liner system is zero. The comparison of solute concentration profiles under two bottom boundary conditions are shown in Fig. 2. The results predicted by the present method and those by Li and Cleall (2011) agree perfectly well. Thus, the present method is able to describe transient contaminant transport in layered porous media.

### **4 Rationality assessment of the hypotheses of semi-infinite bottom boundary condition and steady-state transport processes**

As aforementioned, steady-state processes in GM and GCL and semi-infinite bottom boundary condition are two important assumptions in the existing works, such as Xie et al. (2015a). The rationality of the two assumptions will be deeply investigated in this part. In order to determine the deviation due to the two assumptions, contaminant transport in a GM/GCL/SL composite liner is assessed using the present method and SSM. Because there

exists no fully transient advection-diffusion analytical solution for three-layer composite liners and SSM is the state-of-the-art for this issue, the comparison between the present method and SSM also serves as model verification to a certain extent.

In the comparison, the bottom concentration deviation ratio is defined as  $R = (\bar{C}_b - C_b) / C_b$ , the absolute bottom concentration deviation ratio is defined as  $|R| = |\bar{C}_b - C_b| / C_b$ , where  $\bar{C}_b$  and  $C_b$  are the bottom concentrations calculated by SSM and the present method, respectively. Similarly, the breakthrough time deviation ratio is defined as  $Rt = (\bar{t}_b - t_b) / t_b$ , where  $\bar{t}_b$  and  $t_b$  are the breakthrough time calculated by SSM and the present method, respectively. The breakthrough time is defined as the moment when the contaminant concentration at the bottom of the composite liner (i.e., the bottom of SL) reaches the maximum allowable value and normally it should be greater than 30 years for a landfill site (Chen et al., 2015). It is noteworthy that the SL is infinite in the positive  $z$  direction (see Fig. 1) in SSM, thus the concentration profile obtained by SSM has infinite depth. In order to compare the concentration profiles in a SL with a finite thickness, the concentration profile obtained by SSM is trimmed at  $z = L_{sl}$ .

Toluene (TOL) is selected as the representative organic contaminant in landfill leachate here (Foose et al., 1999, 2001; Kjeldsen et al., 2002; Chen et al., 2009; Xie et al., 2015a, 2015c). The concentration of TOL is assumed to be fixed at 5 mg/L in the landfill leachate. The maximum allowable concentration of TOL in drinking water is 0.7 mg/L in Chinese specifications (Acar and Haider, 1990; Xie et al., 2015c). The frequency of holes,  $m$ , is assumed to be 2.5 holes/ha on the GM. The interface transmissivity between GM and GCL,  $\theta$ , is  $2 \times 10^{-10} \text{ m}^2/\text{s}$  (Xie et al., 2015a). The length of connected wrinkle,  $L_w$ , is assumed to be 500 m (Chappel et al., 2012; Rowe et al., 2012; Xie et al., 2015a). Zero concentration gradient at the bottom boundary is considered. Without special mentioning, the adopted material properties of the composite liner are summarized in Table 1.

#### 4.1 Influence of SL thickness

Four values of SL thickness (0.3, 0.75, 1.5 and 3.0 m) are adopted here. The comparison of concentration profiles calculated by the present method and SSM is illustrated in Fig. 3. The leachate head is 2 m. For  $L_{sl} = 0.3$  m (Fig. 3a), when the elapsed time is small (e.g.,  $t = 1$  year) the concentration calculated by SSM is larger than that calculated by the present method except in the deep part. However, when the elapsed time is large (e.g.,  $t = 2, 5, 10$  years), the result of SSM tends to be smaller than that of the present method. Similar phenomenon can be observed for  $L_{sl} = 0.75$  m (see Fig. 3b), but the difference between the two methods is much smaller and SSM slightly overrates almost the whole concentration profile even for  $t = 2$  years. If the SL is even thicker (e.g.,  $L_{sl} = 1.5$  m), the results of the two methods are very similar except the deep part for  $t = 10$  years. For  $L_{sl} = 3.0$  m, the results of the two methods match very well. It is not strange that the semi-infinite assumption becomes more and more reasonable with the increase of SL thickness.

In order to further investigate the influence of SL thickness, the breakthrough curve is studied (see Fig. 4). When the TOL concentration at the bottom of the composite liner reaches the maximum allowable value (i.e., 0.7 mg/L),  $C_b/C_0$  is 0.14. The breakthrough time for each scenario can be determined based on Fig. 4, and the values are summarized in Table 2. Obviously, except for the composite liner with small  $L_{sl}$ , the breakthrough time is overestimated by SSM. In fact, the difference between the two methods shown in Figs. 3-4 are complicated and synthetically caused by the two assumptions, which will be comprehensively deciphered in Section 4.3.

#### 4.2 Influence of leachate head

Four values of leachate head (0.3, 3, 5 and 10 m) are selected here. The concentration

profiles calculated by the two methods are compared in Fig. 5. The thickness of SL is 0.75 m. As shown in Fig. 5a, when  $h_w = 0.3$  m, the concentration calculated by SSM is larger than that calculated by the present method when the elapsed time is small ( $t = 1, 2$  years), and it is contrary when the elapsed time is large ( $t = 10$  years). Similar law can be observed for the other three scenarios in Fig. 5b, c, d. When the leachate head is large enough (e.g.,  $h_w = 5, 10$  m), the concentration profile is nearly a vertical line when the elapsed time is large enough (e.g.,  $t = 10$  years in Fig. 5c and  $t = 5, 10$  years in Fig. 5d), indicating that the composite liner has completely failed. Similarly, the breakthrough curves predicted by the two methods are compared in Fig. 6, and the breakthrough time is summarized in Table 3. The calculated breakthrough time by SSM gradually changes from overestimation to underestimation with the increase of leachate head.

#### 4.3 Coupling influence of SL thickness and leachate head

To analyze the coupling effect of the two assumptions, composite liner with various SL thicknesses under a range of leachate head is studied in this section. The  $L_{sl}$  ranges from 0 to 3 m and the leachate head ranges from 0 to 10 m.

The variation of the calculated relative bottom concentration by the present method,  $C_b/C_0$ , is shown in Fig. 7, where  $C_b/C_0 < 0.14$  defines the “un-breakthrough zone” and  $C_b/C_0 \geq 0.14$  defines the “breakthrough zone”. As shown in Fig. 7a, when the elapsed time is small (e.g.,  $t = 5$  years in Fig. 7a), the areas of the two zones are almost the same, the breakthrough zone is in the region with high  $h_w$  and low  $L_{sl}$  (i.e., the upper left side), and the un-breakthrough zone is in the region with low  $h_w$  and high  $L_{sl}$  (i.e., the lower right side). With the increase of elapsed time, the boundary between the two zones moves towards the right bottom corner, the area of the un-breakthrough zone decreases gradually (see Fig. 7a, b, c) and is overwhelmed by the breakthrough zone when  $t = 100$  years (see Fig. 7d).

The variation of the absolute bottom concentration deviation ratio,  $|R|$ , is shown in Fig. 8, where  $R > 5\%$  represents the result of SSM is obviously larger than that of the present method, namely, “overestimated zone”; similarly,  $R < -5\%$  represents “underestimated zone” and the rest ( $-5\% \leq R \leq 5\%$ ) is “no difference zone”. The figure shows that there is significant difference between the two methods, especially at the early stage. When the elapsed time is small (e.g.,  $t = 5$  years in Fig. 8a), all the three zones exist. Compared with the overestimated zone, the underestimated zone is much larger. In region with low  $L_{sl}$  and  $h_w$ , the value of  $|R|$  can even reach approximately 50%. Specifically, when  $L_{sl}$  is relatively large, such as 2.5 m, it evolves from the underestimated zone to the no difference zone and then to the overestimated zone with the increase of  $h_w$ . With the increase of elapsed time, the overestimated zone disappears, the area of the underestimated zone decreases gradually (see Fig. 8b, c, d) and is overwhelmed by the no difference zone when  $t = 100$  years, indicating that the steady-state assumption is more and more reasonable with increasing elapsed time. Although the no difference zone is dominant when the elapsed time is large enough, SSM still obviously underestimates the bottom concentration for scenario with low  $h_w$  and medium or large  $L_{sl}$ , which will overestimate the breakthrough time as shown in Tables 2 and 3. Thus, in the no difference zone, the semi-infinite assumption and steady-state assumption are rational, in the other two zones, the two assumptions cause errors. Notably, for common composite liners with  $L_{sl}$  ranging from 1 to 2 m (Chen et al., 2015) under leachate head ranging from 0 to 2 m, the average bottom concentration deviation ratio,  $R$ , is -27% at the interest time of 30 years. Therefore, the two assumptions will lead to significant overestimation of the breakthrough time for the widely used composite liner if the leachate head is below 2 m.

## 5 Equivalency assessment between GM/GCL/SL and GM/CCL composite liners

GCL is a good choice for replacing CCL in landfill liner system because of its low

permeability and low price especially for sites lacking clay (Giroud et al., 1997; Qian et al., 2002; Shan and Lai, 2002; Touze-Foltz et al., 2012). They are generally combined with SL because GCL has particularly small thickness and SL is much cheaper than clay (Guyonnet et al., 2001; Foose, 2010). Notably, an equivalency assessment is required for the two types of composite liner (i.e., GM/GCL/SL and GM/CCL). They are viewed to have equivalent performance if they have the same breakthrough time.

The GM/CCL composite liner with 0.75 m or 1.5 m CCL is chosen to study what SL thickness is needed to make the GM/GCL/SL composite liner have equivalent performance. The material properties of the two types of composite liner are shown in Table 1, except the thickness of SL (i.e.,  $L_{sl}$ ). The breakthrough curves under 0.3 and 3 m leachate heads are illustrated in Fig. 9. For  $h_w = 0.3$  m (see Fig. 9a), the required  $L_{sl}$  is 2.64 m in order to have equivalent performance to GM/CCL composite liner with  $L_{ccl} = 0.75$  m. Similarly, the required  $L_{sl}$  is 5.21 m for  $L_{ccl} = 1.5$  m. For  $h_w = 3$  m (see Fig. 9b), the required  $L_{sl}$  reduces to 1.68 and 3.67 m, respectively. Thus, the GM/GCL/SL composite liner performs better than GM/CCL composite liner under high leachate level.

The influence of the hydraulic conductivity of SL,  $k_{sl}$ , on the performance of the GM/GCL/SL composite liner is investigated in Fig. 10. The left two breakthrough curves reveal that  $k_{sl}$  has little effect on the breakthrough behavior of the GM/GCL/SL composite liner, the reason is that the hydraulic conductivity of the composite liner is dominated by GCL. The adsorption effect in SL is also examined in Fig. 10. The SL and CCL have the same thickness (0.75 m). The distribution coefficient of SL (i.e.,  $K_{d,sl}$ ) needs to reach 1.74 to make the GM/GCL/SL composite liner have the equivalent performance to the GM/CCL composite liner. Moreover, if the SL has no adsorption ability, the required SL thickness is 2.64 m (see Fig. 9a). Hence, the adsorption capacity of SL significantly influences the performance of the composite liner. Similar phenomenon can be observed in GCL and hence

not repeated here. The above analysis demonstrates that the present method is able to properly and readily conduct the equivalency assessment between different composite liners.

## 6 Summary and conclusions

A transient analytical solution for transport of organic contaminants through a GM/GCL/SL composite liner considering finite bottom boundary condition is proposed in this study. The transient diffusion-advection processes in the whole composite liner and adsorption in GCL and SL can be described by the present method. The method is successfully verified against the analytical solution to a coupling transient diffusion-advection problem in double-layer porous media reported by Li and Cleall (2011). Particular attention is paid to the rationality of the semi-infinite bottom boundary assumption and the steady-state transport assumption in GM and GCL, which are widely adopted in the existing works. The equivalency assessment between GM/GCL/SL and GM/CCL composite liners is also conducted. Some major conclusions can be drawn from the results.

(1) The semi-infinite assumption will induce significant errors if the SL thickness is small. Similarly, the steady-state assumption also causes notable errors at the early stage.

(2) The present method is able to identify overestimated zone, underestimated zone and no difference zone under various conditions. In the no difference zone, the two assumptions are rational; while obvious errors can be caused by the two assumptions in the other two zones.

(3) The two assumptions have significant effect on the contaminant concentration profile in the composite liner, especially at the early stage when all the three zones exist. With the increase of elapsed time, the overestimated zone disappears, and the underestimated zone becomes smaller and smaller and finally is overwhelmed by the no difference zone. As a result, the two assumptions would lead to significant overestimation of the breakthrough time

for the widely used composite liner if the leachate head is below 2 m.

(4) GM/GCL/SL composite liner performs better than GM/CCL composite liner under high leachate level condition. The hydraulic conductivity of SL has little effect on the breakthrough behavior of the GM/GCL/SL composite liner, but the adsorption process in SL can substantially influence the performance of the GM/GCL/SL composite liner.

### Acknowledgments

Much of the work described in this paper was supported by the National Natural Science Foundation of China under Grant Nos. 41725012, 41572265 and 41661130153, the Shanghai Shuguang Program under Grant No. 16SG19, the Fundamental Research Funds for the Central Universities, and the Newton Advanced Fellowship of the Royal Society under Grant No. NA150466. The writers would like to greatly acknowledge all these financial supports and express their most sincere gratitude.

### Appendix A. Derivation of the governing equation for GM

There is no sorption and degradation of contaminant in GM. The mass conservation equation of a representative element is given by

$$\frac{\partial C_{\text{gm}}(z, t)}{\partial t} = -\frac{\partial f(z, t)}{\partial z} \quad (\text{A.1})$$

where  $f(z, t)$  is the mass flux through the representative element at any position  $z$  and any time  $t$ , which is

$$f(z, t) = f_{\text{d}}(z, t) + f_{\text{a}}(z, t) \quad (\text{A.2})$$

where  $f_{\text{d}}(z, t)$  is the mass flux of contaminant diffusion through the intact GM and  $f_{\text{a}}(z, t)$  is the mass flux of contaminant advection through the defects and holes in GM.  $f_{\text{d}}(z, t)$  is given by

$$f_{\text{d}}(z, t) = D_{\text{gm}} \frac{\partial C_{\text{gm}}(z, t)}{\partial z} \quad (\text{A.3})$$

and  $f_a(z, t)$  is given by

$$f_a(z, t) = v_a \frac{C_{gm}(z, t)}{K_g} \quad (\text{A.4})$$

Now substituting Eqs. (A.3) and (A.4) into Eq. (A.2), then employing the result in Eq. (A.1), the governing equation for contaminant transport through GM can be rewritten as

$$\frac{\partial C_{gm}(z, t)}{\partial t} = D_{gm} \frac{\partial^2 C_{gm}(z, t)}{\partial z^2} - \frac{v_a}{K_g} \frac{\partial C_{gm}(z, t)}{\partial z} \quad (\text{A.5})$$

### Appendix B. Solution to $u_i(z)$

The governing equation for the sub-problem 1 is

$$\frac{D_i}{R_{d,i}} \frac{d^2 u_i(z)}{dz^2} - \frac{v_i}{R_{d,i}} \frac{du_i(z)}{dz} = 0, \quad i = 1, 2, 3 \quad (\text{B.1})$$

The top boundary condition is

$$u_1(z)|_{z=0} = C_0 \quad (\text{B.2})$$

The continuity conditions at the interface between GM and GCL are

$$u_1(z)|_{z=L_1/K_g} = u_2(z)|_{z=L_1/K_g} \quad (\text{B.3})$$

$$D_1 \frac{\partial u_1(z)}{\partial z} \Big|_{z=L_1/K_g} = n_2 D_2 \frac{\partial u_2(z)}{\partial z} \Big|_{z=L_1/K_g} \quad (\text{B.4})$$

The continuity conditions at the interface between GCL and SL are

$$u_2(z)|_{z=L_1/K_g+L_2} = u_3(z)|_{z=L_1/K_g+L_2} \quad (\text{B.5})$$

$$n_2 D_2 \frac{\partial u_2(z)}{\partial z} \Big|_{z=L_1/K_g+L_2} = n_3 D_3 \frac{\partial u_2(z)}{\partial z} \Big|_{z=L_1/K_g+L_2} \quad (\text{B.6})$$

The potential bottom boundary conditions are

$$u_3(z)|_{z=H} = 0 \quad (\text{for the Dirichlet boundary}) \quad (\text{B.7})$$

$$\left. \frac{\partial u_3(z)}{\partial z} \right|_{z=H} = 0 \quad (\text{for the Neumann boundary}) \quad (\text{B.8})$$

where

$$H = L_1 / K_g + L_2 + L_3 \quad (\text{B.9})$$

Obviously, the solution to Eq. (B.1) satisfying all the relevant boundary conditions is

$$u_i(z) = k_{i,1} e^{r_{i,1} z} + k_{i,2} e^{r_{i,2} z}, \quad i = 1, 2, 3 \quad (\text{B.10})$$

where  $k_{i,1}$ ,  $k_{i,2}$ ,  $r_{i,1}$  and  $r_{i,2}$  can be obtained using the boundary and continuity conditions (Eqs. (B.2)-(B.9)).

### Appendix C. Solution to $w_i(z, t)$

The governing equation for the sub-problem 2 is

$$\frac{\partial w_i(z, t)}{\partial t} = \frac{D_i}{R_{d,i}} \frac{\partial^2 w_i(z, t)}{\partial z^2} - \frac{v_i}{R_{d,i}} \frac{\partial w_i(z, t)}{\partial z}, \quad i = 1, 2, 3 \quad (\text{C.1})$$

The top boundary condition is

$$w_1(z, t) \Big|_{z=0} = 0 \quad (\text{C.2})$$

The continuity conditions at the interface between GM and GCL are

$$w_1(z, t) \Big|_{z=L_1/K_g} = w_2(z, t) \Big|_{z=L_1/K_g} \quad (\text{C.3})$$

$$D_1 \frac{\partial w_1(z, t)}{\partial z} \Big|_{z=L_1/K_g} = n_2 D_2 \frac{\partial w_2(z, t)}{\partial z} \Big|_{z=L_1/K_g} \quad (\text{C.4})$$

The continuity conditions at the interface between GCL and SL are

$$w_2(z, t) \Big|_{z=L_1/K_g+L_2} = w_3(z, t) \Big|_{z=L_1/K_g+L_2} \quad (\text{C.5})$$

$$n_2 D_2 \frac{\partial w_2(z, t)}{\partial z} \Big|_{z=L_1/K_g+L_2} = n_3 D_3 \frac{\partial w_3(z, t)}{\partial z} \Big|_{z=L_1/K_g+L_2} \quad (\text{C.6})$$

The potential bottom boundary conditions are

$$w_3(z, t)|_{z=H} = 0 \quad (\text{for the Dirichlet boundary}) \quad (\text{C.7})$$

$$\left. \frac{\partial w_3(z, t)}{\partial z} \right|_{z=H} = 0 \quad (\text{for the Neumann boundary}) \quad (\text{C.8})$$

The initial condition is

$$w_i(z, 0) = 0, \quad i = 1, 2, 3 \quad (\text{C.9})$$

Based on separation of variables method, the solution to Eq. (C.1) satisfying all the relevant conditions can be expressed as

$$w_i(z, t) = \sum_{m=1}^{\infty} C_m g_{m,i}(z) e^{a_i z - \beta_m t}, \quad i = 1, 2, 3 \quad (\text{C.10})$$

When  $\beta_m - v_i^2/(4D_i R_{d,i}) \geq 0$ ,

$$g_{m,i}(z) = A_{m,i} \sin(\mu_i \lambda_{m,i} z) + B_{m,i} \cos(\mu_i \lambda_{m,i} z); \quad i = 1, 2, 3 \quad (\text{C.11a})$$

When  $\beta_m - v_i^2/(4D_i R_{d,i}) < 0$ ,

$$g_{m,i}(z) = A_{m,i} \sinh(\mu_i \lambda_{m,i} z) + B_{m,i} \cosh(\mu_i \lambda_{m,i} z); \quad i = 1, 2, 3 \quad (\text{C.11b})$$

Substituting Eqs. (C.10) and (C.11) into Eq. (C.1), the coefficients  $a_i$  and  $\lambda_{m,i}$  can be obtained:

$$a_i = \frac{v_i}{2D_i}, \quad i = 1, 2, 3 \quad (\text{C.12})$$

$$\lambda_{m,i} = \sqrt{\frac{R_{d,1}}{D_1} \left| \beta_m - \frac{v_i^2}{4D_i R_{d,i}} \right|}, \quad i = 1, 2, 3 \quad (\text{C.13})$$

and the coefficient  $\mu_i$  is defined as

$$\mu_i = \sqrt{\frac{R_{d,i}/D_i}{R_{d,1}/D_1}}, \quad i = 1, 2, 3 \quad (\text{C.14})$$

Substituting Eqs. (C.10) and (C.11) into the continuity conditions (Eqs. (C.3)-(C.6)), the coefficients  $A_{m,i}$  and  $B_{m,i}$  can be determined by the following recursive equation:

$$\begin{bmatrix} A_{m,i} \\ B_{m,i} \end{bmatrix} = T_{i-1} \begin{bmatrix} A_{m,i-1} \\ B_{m,i-1} \end{bmatrix}, \quad i = 2, 3 \quad (\text{C.15})$$

where the transfer matrix  $T_i$  can be determined by

$$T_i = \frac{e^{(a_i - a_{i+1})z_i}}{n_{i+1}D_{i+1}\mu_{i+1}\lambda_{m,i+1}} \begin{bmatrix} \bar{C}_i\bar{F}_i - \bar{B}_i\bar{G}_i & \bar{C}_i\bar{H}_i - \bar{D}_i\bar{G}_i \\ \bar{B}_i\bar{E}_i - \bar{A}_i\bar{F}_i & \bar{D}_i\bar{E}_i - \bar{A}_i\bar{H}_i \end{bmatrix}, \quad i = 1, 2 \quad (\text{C.16})$$

In above, when  $\beta_m - v_i^2/(4D_iR_{d,i}) \geq 0$  and  $\beta_m - v_{i+1}^2/(4D_{i+1}R_{d,i+1}) \geq 0$ ,

$$\left. \begin{aligned} \bar{A}_i &= \sin(\mu_{i+1}\lambda_{m,i+1}z_i) \\ \bar{B}_i &= \sin(\mu_i\lambda_{m,i}z_i) \\ \bar{C}_i &= \cos(\mu_{i+1}\lambda_{m,i+1}z_i) \\ \bar{D}_i &= \cos(\mu_i\lambda_{m,i}z_i) \\ \bar{E}_i &= n_{i+1}D_{i+1}\mu_{i+1}\lambda_{m,i+1} \cos(\mu_{i+1}\lambda_{m,i+1}z_i) + n_{i+1}D_{i+1}a_{i+1}H \sin(\mu_{i+1}\lambda_{m,i+1}z_i) \\ \bar{F}_i &= n_iD_i\mu_i\lambda_{m,i} \cos(\mu_i\lambda_{m,i}z_i) + n_iD_ia_iH \sin(\mu_i\lambda_{m,i}z_i) \\ \bar{G}_i &= n_{i+1}D_{i+1}a_{i+1}H \cos(\mu_{i+1}\lambda_{m,i+1}z_i) - n_{i+1}D_{i+1}\mu_{i+1}\lambda_{m,i+1} \sin(\mu_{i+1}\lambda_{m,i+1}z_i) \\ \bar{H}_i &= n_iD_ia_iH \cos(\mu_i\lambda_{m,i}z_i) - n_iD_i\mu_i\lambda_{m,i} \sin(\mu_i\lambda_{m,i}z_i) \end{aligned} \right\}, \quad i = 1, 2 \quad (\text{C.17a})$$

when  $\beta_m - v_i^2/(4D_iR_{d,i}) \geq 0$  and  $\beta_m - v_{i+1}^2/(4D_{i+1}R_{d,i+1}) < 0$ ,

$$\left. \begin{aligned} \bar{A}_i &= \sinh(\mu_{i+1}\lambda_{m,i+1}z_i) \\ \bar{B}_i &= \sin(\mu_i\lambda_{m,i}z_i) \\ \bar{C}_i &= \cosh(\mu_{i+1}\lambda_{m,i+1}z_i) \\ \bar{D}_i &= \cos(\mu_i\lambda_{m,i}z_i) \\ \bar{E}_i &= n_{i+1}D_{i+1}\mu_{i+1}\lambda_{m,i+1} \cosh(\mu_{i+1}\lambda_{m,i+1}z_i) + n_{i+1}D_{i+1}a_{i+1}H \sinh(\mu_{i+1}\lambda_{m,i+1}z_i) \\ \bar{F}_i &= n_iD_i\mu_i\lambda_{m,i} \cos(\mu_i\lambda_{m,i}z_i) + n_iD_ia_iH \sin(\mu_i\lambda_{m,i}z_i) \\ \bar{G}_i &= n_{i+1}D_{i+1}a_{i+1}H \cosh(\mu_{i+1}\lambda_{m,i+1}z_i) - n_{i+1}D_{i+1}\mu_{i+1}\lambda_{m,i+1} \sinh(\mu_{i+1}\lambda_{m,i+1}z_i) \\ \bar{H}_i &= n_iD_ia_iH \cos(\mu_i\lambda_{m,i}z_i) - n_iD_i\mu_i\lambda_{m,i} \sin(\mu_i\lambda_{m,i}z_i) \end{aligned} \right\}, \quad i = 1, 2 \quad (\text{C.17b})$$

when  $\beta_m - v_i^2/(4D_iR_{d,i}) < 0$  and  $\beta_m - v_{i+1}^2/(4D_{i+1}R_{d,i+1}) \geq 0$ ,

$$\left. \begin{aligned}
 \bar{A}_i &= \sin(\mu_{i+1}\lambda_{m,i+1}z_i) \\
 \bar{B}_i &= \sinh(\mu_i\lambda_{m,i}z_i) \\
 \bar{C}_i &= \cos(\mu_{i+1}\lambda_{m,i+1}z_i) \\
 \bar{D}_i &= \cosh(\mu_i\lambda_{m,i}z_i) \\
 \bar{E}_i &= n_{i+1}D_{i+1}\mu_{i+1}\lambda_{m,i+1}\cos(\mu_{i+1}\lambda_{m,i+1}z_i) + n_{i+1}D_{i+1}a_{i+1}H\sin(\mu_{i+1}\lambda_{m,i+1}z_i) \\
 \bar{F}_i &= n_iD_i\mu_i\lambda_{m,i}\cosh(\mu_i\lambda_{m,i}z_i) + n_iD_ia_iH\sinh(\mu_i\lambda_{m,i}z_i) \\
 \bar{G}_i &= n_{i+1}D_{i+1}a_{i+1}H\cos(\mu_{i+1}\lambda_{m,i+1}z_i) - n_{i+1}D_{i+1}\mu_{i+1}\lambda_{m,i+1}\sin(\mu_{i+1}\lambda_{m,i+1}z_i) \\
 \bar{H}_i &= n_iD_ia_iH\cosh(\mu_i\lambda_{m,i}z_i) - n_iD_i\mu_i\lambda_{m,i}\sinh(\mu_i\lambda_{m,i}z_i)
 \end{aligned} \right\}, i = 1, 2 \quad (\text{C.17c})$$

when  $\beta_m - v_i^2/(4D_iR_{d,i}) < 0$  and  $\beta_m - v_{i+1}^2/(4D_{i+1}R_{d,i+1}) < 0$ ,

$$\left. \begin{aligned}
 \bar{A}_i &= \sinh(\mu_{i+1}\lambda_{m,i+1}z_i) \\
 \bar{B}_i &= \sinh(\mu_i\lambda_{m,i}z_i) \\
 \bar{C}_i &= \cosh(\mu_{i+1}\lambda_{m,i+1}z_i) \\
 \bar{D}_i &= \cosh(\mu_i\lambda_{m,i}z_i) \\
 \bar{E}_i &= n_{i+1}D_{i+1}\mu_{i+1}\lambda_{m,i+1}\cosh(\mu_{i+1}\lambda_{m,i+1}z_i) + n_{i+1}D_{i+1}a_{i+1}H\sinh(\mu_{i+1}\lambda_{m,i+1}z_i) \\
 \bar{F}_i &= n_iD_i\mu_i\lambda_{m,i}\cosh(\mu_i\lambda_{m,i}z_i) + n_iD_ia_iH\sinh(\mu_i\lambda_{m,i}z_i) \\
 \bar{G}_i &= n_{i+1}D_{i+1}a_{i+1}H\cosh(\mu_{i+1}\lambda_{m,i+1}z_i) - n_{i+1}D_{i+1}\mu_{i+1}\lambda_{m,i+1}\sinh(\mu_{i+1}\lambda_{m,i+1}z_i) \\
 \bar{H}_i &= n_iD_ia_iH\cosh(\mu_i\lambda_{m,i}z_i) - n_iD_i\mu_i\lambda_{m,i}\sinh(\mu_i\lambda_{m,i}z_i)
 \end{aligned} \right\}, i = 1, 2 \quad (\text{C.17d})$$

Substituting Eqs. (C.10) and (C.11) into the bottom boundary condition (Eqs. (C.7) and (C.8)), the eigenvalues  $\beta_m$  can be determined by the characteristic equation:

$$T_3T_2T_1T_0 = 0 \quad (\text{C.18})$$

in which, for the Dirichlet boundary

$$T_3 = \begin{cases} [\sin(\mu_3\lambda_{m,3}H) \cos(\mu_3\lambda_{m,3}H)]; & \text{when } \beta_m - \frac{v_i^2}{4D_iR_{d,i}} \geq 0 \\ [\sinh(\mu_3\lambda_{m,3}H) \cosh(\mu_3\lambda_{m,3}H)]; & \text{when } \beta_m - \frac{v_i^2}{4D_iR_{d,i}} < 0 \end{cases} \quad (\text{C.19})$$

and for the Neumann boundary

$$T_3 = \begin{cases} \begin{bmatrix} \mu_3 \lambda_{m,3} \cos(\mu_3 \lambda_{m,3} H) + a_3 \sin(\mu_3 \lambda_{m,3} H) \\ -\mu_3 \lambda_{m,3} \sin(\mu_3 \lambda_{m,3} H) + a_3 \cos(\mu_3 \lambda_{m,3} H) \end{bmatrix}^T; & \text{when } \beta_m - \frac{v_i^2}{4D_i R_{d,i}} \geq 0 \\ \begin{bmatrix} \mu_3 \lambda_{m,3} \cosh(\mu_3 \lambda_{m,3} H) + a_3 \sinh(\mu_3 \lambda_{m,3} H) \\ \mu_3 \lambda_{m,3} \sinh(\mu_3 \lambda_{m,3} H) + a_3 \cosh(\mu_3 \lambda_{m,3} H) \end{bmatrix}^T; & \text{when } \beta_m - \frac{v_i^2}{4D_i R_{d,i}} < 0 \end{cases} \quad (\text{C.20})$$

$T_0$  can be obtained by substituting Eqs. (C.10) and (C.11) into the top boundary condition (Eq. (C.2)):

$$T_0 = [A_{m,1} \ B_{m,1}]^T = [1 \ 0]^T \quad (\text{C.21})$$

Consequently, all the coefficients in the function  $g_{m,i}(z)$  can be determined.

Finally, the coefficient  $C_m$  in the solution to the sub-problem 2 can be determined by the orthogonality condition:

$$C_m = - \frac{\int_0^{z_1} u_1(z) n_1 R_{d,1} g_{m,1}(z) e^{-a_1 z} dz + \int_{z_1}^{z_2} u_2(z) n_2 R_{d,2} S_1 g_{m,2}(z) e^{-a_2 z} dz + \int_{z_2}^{z_3} u_3(z) n_3 R_{d,3} S_2 g_{m,3}(z) e^{-a_3 z} dz}{\int_0^{z_1} n_1 R_{d,1} g_{m,1}^2(z) dz + \int_{z_1}^{z_2} n_2 R_{d,2} S_1 g_{m,2}^2(z) dz + \int_{z_2}^{z_3} n_3 R_{d,3} S_2 g_{m,3}^2(z) dz} \quad (\text{C.22})$$

in which

$$\left. \begin{aligned} S_1 &= e^{2(a_2 - a_1)z_1} \\ S_2 &= e^{-2z_1 a_1 + 2(z_1 - z_2)a_2 + 2z_2 a_3} \end{aligned} \right\} \quad (\text{C.23})$$

**References**

- Acar, Y.B., Haider, L., 1990. Transport of low-concentration contaminants in saturated earthen barriers. *J. Geotech. Eng.* 116(7), 1031-1052.
- Barroso, M., Touze-Foltz, N., Von Maubeuge, K., Pierson, P., 2006. Laboratory investigation of flow rate through composite liners consisting of a geomembrane, a GCL and a soil liner. *Geotext. Geomembr.* 24(3), 139-155.
- Benson, C.H., Daniel, D.E., Boutwell, G.P., 1999. Field performance of compacted clay liners. *J. Geotech. Geoenviron. Eng.* 125(5), 390-403.
- Bouazza, A., Bowders Jr., J., 2010. *Geosynthetic clay liners for waste containment facilities.* CRC Press/Balkema, Taylor and Francis Group, Leiden, Netherlands, p. 239.
- Chappel, M.J., Rowe, R.K., Brachman, R.W. I., Take, W.A., 2012. A comparison of geomembrane wrinkles for nine field cases. *Geosynth. Int.* 19(6), 453-469.
- Chen, Y., Xie, H., Ke, H., Chen, R., 2009. An analytical solution for one-dimensional contaminant diffusion through multi-layered system and its applications. *Environ. Geol.* 58(5), 1083-1094.
- Chen, Y., Wang, Y., Xie, H., 2015. Breakthrough time-based design of landfill composite liners. *Geotext. Geomembr.* 43(2), 196-206.
- Cleall, P.J., Li, Y.C., 2011. Analytical solution for diffusion of VOCs through composite landfill liners. *J. Geotech. Geoenviron. Eng.* 137, 850-854.
- Du, Y.J., Shen, S.L., Liu, S.Y., Hayashi, S., 2009. Contaminant mitigating performance of Chinese standard municipal solid waste landfill liner systems. *Geotext. Geomembr.* 27(3), 232-239.
- Edil, T.B., 2003. A review of aqueous-phase VOC transport in modern landfill liners. *Waste Manage.* 23, 561-571.
- El-Zein, A., 2008. A general approach to the modelling of contaminant transport through

- composite landfill liners with intact or leaking geomembranes. *Int. J. Numer. Anal. Met. Geomech.* 32 (3), 265-287.
- El-Zein, A., McCarroll, I., Touze-Foltz, N., 2012. Three-dimensional finite-element analyses of seepage and contaminant transport through composite geosynthetic clay liners with multiple defects. *Geotext. Geomembr.* 33, 34-42.
- Foose, G.J., Benson, C.H., Edil, T.B., 1999. Equivalency of composite geosynthetic clay liners as a barrier to volatile organic compounds. In: *Proceedings Geosynthetics*, Saint Paul, April, pp. 321-334.
- Foose, G.J., Benson, C.H., Edil, T.B., 2001. Analytical equations for predicting concentration and mass flux from composite liners. *Geosyn. Int.* 8(6), 551-575.
- Foose, G.J., 2002. Transit-time design for diffusion through composite liners. *J. Geotech. Geoenviron. Eng.* 128: 590-601.
- Foose, G.J., 2010. A steady-state approach for evaluating the impact of solute transport through composite liners on groundwater quality. *Waste Manage.* 30(8), 1577-1586.
- Giroud, J.P., Badu-Tweneboah, K., Soderman, K.L., 1997. Comparison of leachate flow through compacted clay liners in landfill liner systems. *Geosyn. Int.* 4(3-4), 391-431.
- Guan, C., Xie, H.J., Wang, Y.Z., Chen, Y.M., Jiang, Y.S., Tang, X.W., 2014. An analytical model for solute transport through a GCL-based two-layered liner considering biodegradation. *Sci. Total Environ.* 466, 221-231.
- Guerrero, J.P., Pontedeiro, E.M., van Genuchten, M.T., Skaggs, T.H., 2013. Analytical solutions of the one-dimensional advection–dispersion solute transport equation subject to time-dependent boundary conditions. *Chem. Eng. J.* 221, 487-491.
- Guerrero, J.P., Skaggs, T.H., 2010. Analytical solution for one-dimensional advection-dispersion transport equation with distance-dependent coefficients. *J. Hydrol.* 390, 57-65.

- Guyonnet, D., Perrochet, P., Côme, B., Seguin, J.J., Parriaux, A., 2001. On the hydro-dispersive equivalence between multi-layered mineral barriers. *J. Contam. Hydrol.* 51(3-4), 215-231.
- Han, Z., Ma, H., Shi, G., He, L., Wei, L., Shi, Q., 2016. A review of groundwater contamination near municipal solid waste landfill sites in China. *Sci. Total Environ.* 569, 1255-1264.
- Hoor, A., Rowe, R.K., 2013. Potential for desiccation of geosynthetic clay liners used in barrier systems. *J. Geotech. Geoenviron. Eng.* 139(10), 1648-1664.
- Islam, M.Z., Rowe, R.K., 2008. Effect of geomembrane ageing on the diffusion of VOCs through HDPE geomembranes. In: *Geoamericas 2008*, Cancun, Mexico, March, pp. 459-467.
- Kjeldsen, P., Barlaz, M.A., Rooker, A.P., Baun, A., Ledin, A., Christensen, T.H., 2002. Present and long-term composition of MSW landfill leachate. *Environ. Sci. Technol.* 32(4), 297-336.
- Lake, C.B., Rowe, R.K., 2005. A comparative assessment of volatile organic compound (VOC) sorption to various types of potential GCL bentonites. *Geotext. Geomembr.* 23(4), 323-347.
- Leo, A., Hansch, C., Elkins, D., 1971. Partition coefficients and their uses. *Chem. Rev.* 71(6), 525-616.
- Li, Y.C., Cleall, P.J., 2011. Analytical solutions for advective–dispersive solute transport in double-layered finite porous media. *Int. J. Numer. Anal. Met. Geomech.* 35(4), 438-460.
- Liu, C., Ball, W.P., 1998. Analytical modeling of diffusion-limited contamination and decontamination in a two-layer porous medium. *Adv. Water Resour.* 21(4), 297-313.
- Liu, G., Barbour, L., Si, B. C., 2009. Unified multilayer diffusion model and application to diffusion experiment in porous media by method of chambers. *Environ. Sci. Technol.*

- 43(7), 2412-2416.
- Park, M.G., Edil, T.B., Benson, C.H., 2012. Modeling volatile organic compound transport in composite liners. *J. Geotech. Geoenviron. Eng.* 138(6), 641-657.
- Postigo, C., Martinez, D.E., Grondona, S. and Miglioranza, K.S.B., 2018. Groundwater pollution: sources, mechanisms, and prevention. *The Encyclopedia of the Anthropocene*, vol. 5, p. 87-96. Oxford, Elsevier, New York, USA.
- Qian, X., Koerner, R.M., Gray, D.H., 2002. *Geotechnical aspects of landfill design and construction*. Prentice Hall, New Jersey, USA, p. 717.
- Qiu, J., 2011. China to spend billions cleaning up groundwater. *Science*, 334(11), 745.
- Rowe, R.K., 1998. Geosynthetics and the minimization of contaminant migration through barrier systems beneath solid waste. Keynote paper. In: *Proceedings of the 6th International Conference on Geosynthetics*, Atlanta, March, pp. 27-103.
- Rowe, R.K., Brachman, R.W.I., 2004. Assessment of equivalence of composite liners. *Geosyn. Int.* 11(4), 273-286.
- Rowe, R.K., 2012. Short- and long-term leakage through composite liners. The 7th Arthur Casagrande Lecture. *Can. Geotech. J.* 49 (2), 141-169.
- Rowe, R.K., Chappel, M.J., Brachman, R.W.I., Take, W.A., 2012. Field study of wrinkles in a geomembrane at a composite liner test site. *Can. Geotech. J.* 49(10), 1196-1211.
- Rowe, R.K., Abdelatty, K., 2013. Leakage and contaminant transport through a single hole in the geomembrane component of a composite liner. *J. Geotech. Geoenviron. Eng.* 139(3), 357-366.
- Sangam, H.P., Rowe, R.K., 2005. Effect of surface fluorination on diffusion through a high density polyethylene geomembrane. *J. Geotech. Geoenviron. Eng.* 131(6), 694-704.
- Shackelford, C.D., Lee, J.M., 2005. Analyzing diffusion by analogy with consolidation. *J. Geotech. Geoenviron. Eng.* 131(11), 1345-1359.

- Shan, H.Y., Lai, Y.J., 2002. Effect of hydrating liquid on the hydraulic properties of geosynthetic clay liners. *Geotext. Geomembr.* 20(1), 19-38.
- Singh, M.K., Das, P., 2015. Scale dependent solute dispersion with linear isotherm in heterogeneous medium. *J. Hydrol.* 520, 289-299.
- Singh, M.K., Chatterjee, A., Singh, V.P., 2017. Solution of one-dimensional time fractional advection dispersion equation by homotopy analysis method. *J. Eng. Mech.* 143(9), 0401-7103.
- Stark, T.D., 2017. Evaluation of a four-component composite landfill liner system. *Environ. Geotech.* 4(4), 257-273.
- Touze-Foltz, N., Zanzinger, H., Koerner, R.M., 2012. Special issue on GCLs. *Geotext. Geomembr.* 33(33), 1
- Varank, G., Demir, A., Top, S., Sekman, E., Akkaya, E., Yetilmezsoy, K., Bilgili, M.S., 2011a. Migration behavior of landfill leachate contaminants through alternative composite liners. *Sci. Total Environ.* 409(17), 3183-3196.
- Varank, G., Demir, A., Yetilmezsoy, K., Bilgili, M.S., Top, S., Sekman, E., 2011b. Estimation of transport parameters of phenolic compounds and inorganic contaminants through composite landfill liners using one-dimensional mass transport model. *Waste Manage.* 31(11), 2263-2274.
- Xie, H., Jiang, Y., Zhang, C., Feng, S., 2015a. An analytical model for volatile organic compound transport through a composite liner consisting of a geomembrane, a GCL, and a soil liner. *Environ. Sci. Pollut. Res.* 22(4), 2824-2836.
- Xie, H., Jiang, Y., Zhang, C., Feng, S., Qiu, Z., 2015b. Steady-state analytical models for performance assessment of landfill composite liners. *Environ. Sci. Pollut. Res.* 22(16), 12198-12214.
- Xie, H., Thomas, H.R., Chen, Y., Sedighi, M., Zhan, T. L., Tang, X., 2015c. Diffusion of

organic contaminants in triple-layer composite liners: an analytical modeling approach.

Acta Geotech. 10(2), 255-262.

Zhan, L.T., Zeng, X., Li, Y., Chen, Y., 2013. Analytical solution for one-dimensional diffusion of organic pollutants in a geomembrane-bentonite composite barrier and parametric analyses. J. Environ. Eng. 140(1), 57-68.

ACCEPTED MANUSCRIPT

## List of Captions

### Table Captions

**Table 1** Material properties of the composite liner.

**Table 2** Breakthrough time (unit: year) of the composite liner with different SL thicknesses.

**Table 3** Breakthrough time (unit: year) of the composite liner under different leachate levels.

### Figure Captions

**Fig. 1.** Mathematical model for contaminant transport through composite liner.

**Fig. 2.** Comparison between the present method with that reported by Li and Cleall (2011) in terms of solute concentration profiles in the double-layer soils: (a) zero concentration at the bottom boundary; (b) zero concentration gradient at the bottom boundary.

**Fig. 3.** Comparison between the present method and SSM in terms of contaminant concentration profiles in the composite liner: (a)  $L_{sl} = 0.3$  m; (b)  $L_{sl} = 0.75$  m; (c)  $L_{sl} = 1.5$  m; (d)  $L_{sl} = 3$  m.

**Fig. 4.** Breakthrough curves of composite liner with different SL thicknesses.

**Fig. 5.** Comparison between the present method and SSM in terms of contaminant concentration profiles in the composite liner: (a)  $h_w = 0.3$  m; (b)  $h_w = 3$  m; (c)  $h_w = 5$  m; (d)  $h_w = 10$  m.

**Fig. 6.** Breakthrough curves of composite liner with different leachate heads.

**Fig. 7.** Calculated relative bottom concentration: (a)  $t = 5$  years; (b)  $t = 15$  years; (c)  $t = 30$  years; (d)  $t = 100$  years.

**Fig. 8.** Absolute bottom concentration deviation ratio: (a)  $t = 5$  years; (b)  $t = 15$  years; (c)  $t = 30$  years; (d)  $t = 100$  years.

**Fig. 9.** Breakthrough curves for GM/CCL and GM/GCL/SL composite liners: (a)  $h_w = 0.3$  m; (b)  $h_w = 3$  m.

**Fig. 10.** Influence of  $k_{sl}$  and  $K_{d,sl}$  on the breakthrough curve of GM/GCL/SL composite liner.

**Table 1** Material properties of the composite liner.

Parameter	GM	GCL	SL	CCL
Thickness, $L$ (m)	0.0015	0.01	0.75	0.75, 1.5
Porosity, $n$	-	0.7	0.3	0.35
Dry density, $\rho_d$ (g/cm <sup>3</sup> )	-	0.79	1.62	1.66
Hydraulic conductivity, $k$ ( $\times 10^{-10}$ m/s)	-	0.5	1000	10
Effective diffusion coefficient, $D$ ( $\times 10^{-10}$ m <sup>2</sup> /s)	0.003	3.00	8.00	4.1
Distribution coefficient, $K_d$ (mL/g)	-	0	0	1.86
Partition coefficient or Henry's coefficient, $K_g$	100	-	-	-

**Table 2** Breakthrough time (unit: year) of the composite liner with different SL thicknesses.

$L_{sl}$	0.3 m	0.75 m	1.5 m	3 m
Xie et al. (2015a)	0.62	2.89	8.40	22.61
This paper	0.63	2.59	7.58	21.05
$dt_b$	-0.01	0.30	0.82	1.56
$Rt$	-3%	12%	11%	7%

Note:  $Rt = dt_b / t_b$ ;  $dt_b = \bar{t}_b - t_b$

**Table 3** Breakthrough time (unit: year) of the composite liner under different leachate levels.

$h_w$	0.3 m	3 m	5 m	10 m
Xie et al. (2015a)	4.56	2.41	1.82	1.14
This paper	3.50	2.26	1.81	1.23
$dt_b$	1.06	0.15	0.01	-0.09
$Rt$	30%	7%	0%	-7%

Note:  $Rt = dt_b / t_b$ ;  $dt_b = \bar{t}_b - t_b$

**Highlights:**

- Analytical solution is given for solute transport in GM/GCL/SL composite liner.
- The transient diffusion-advection processes in composite liner can be simulated.
- The rationality of the steady-state and semi-infinite assumptions are studied.
- The two assumptions cause overestimation of breakthrough time.
- The method is able to properly conduct the equivalency assessment.

ACCEPTED MANUSCRIPT

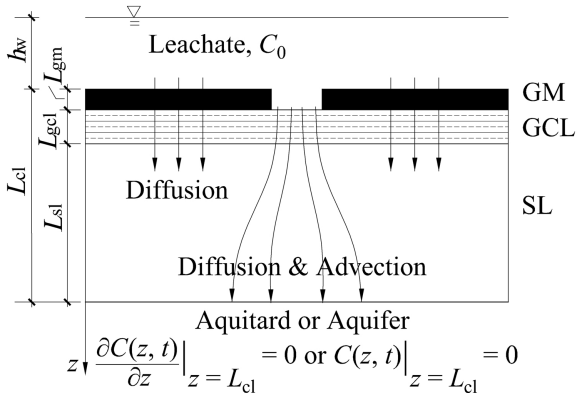


Figure 1

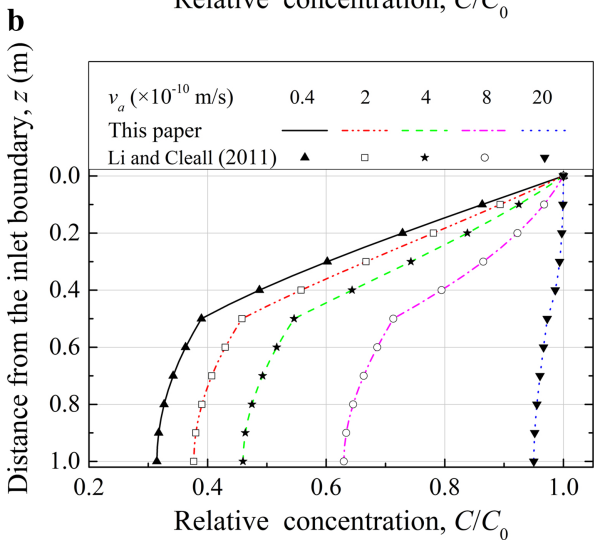
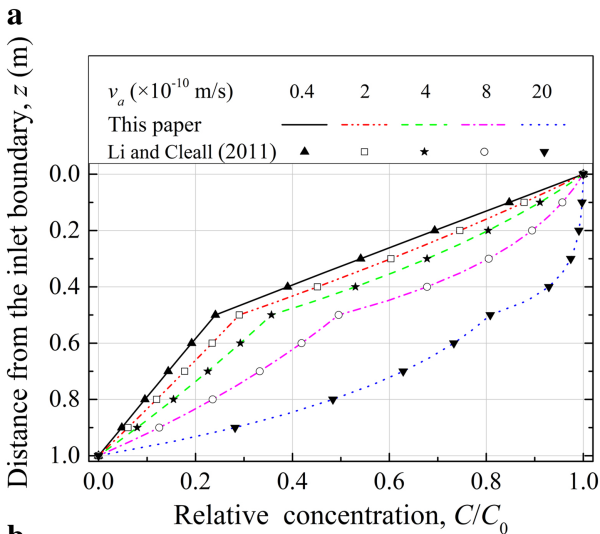


Figure 2

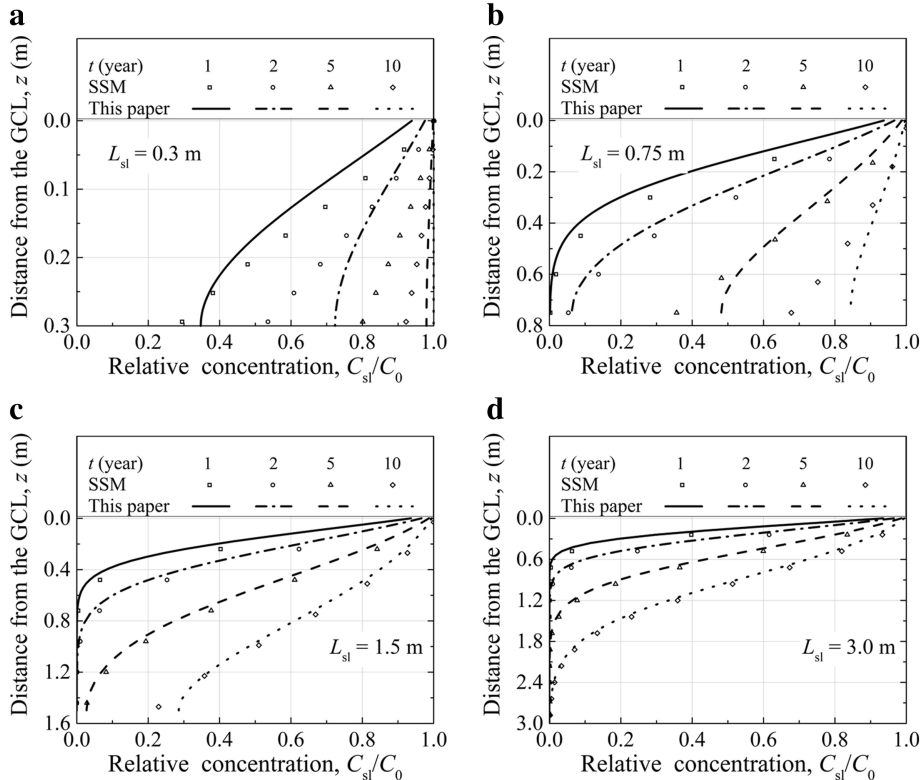


Figure 3

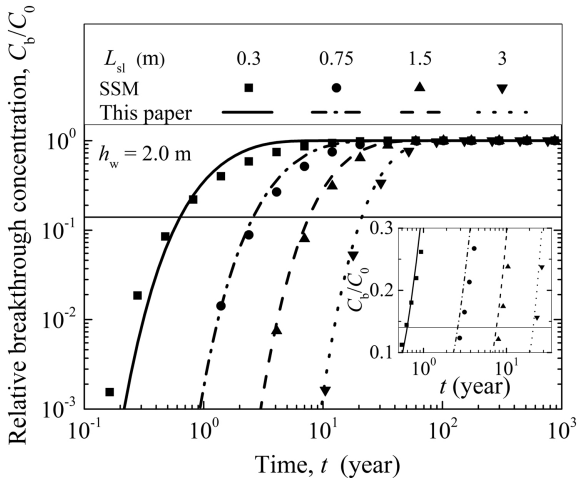


Figure 4

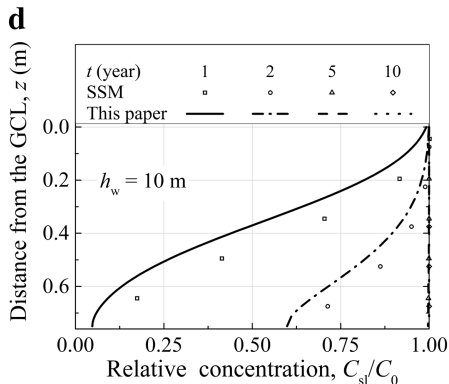
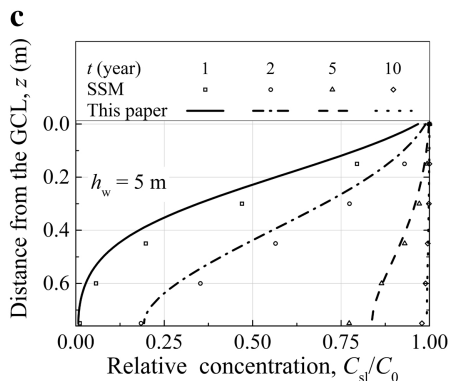
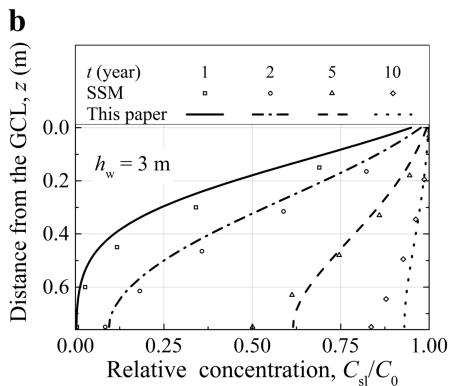
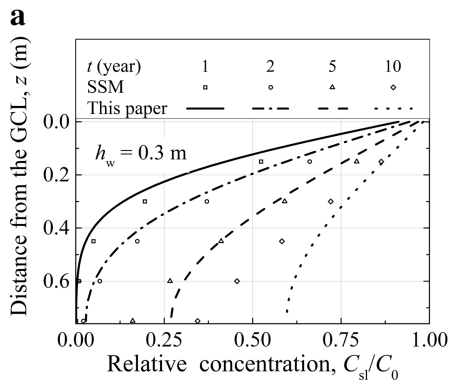


Figure 5

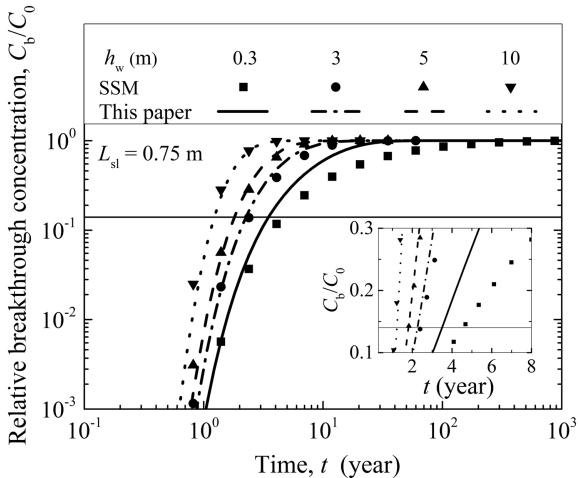


Figure 6

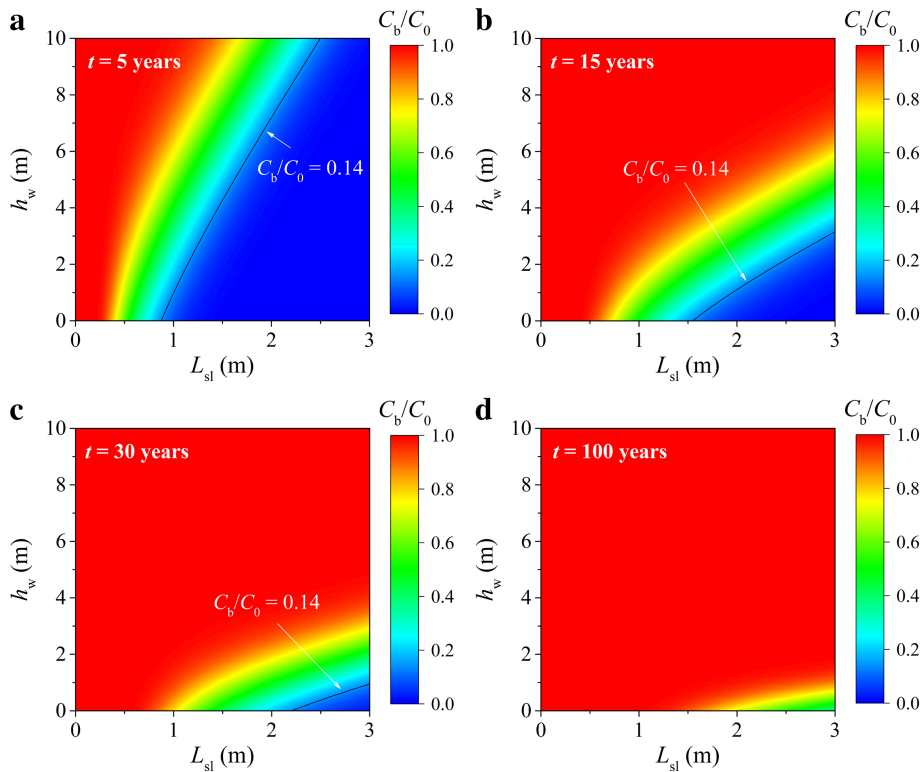


Figure 7

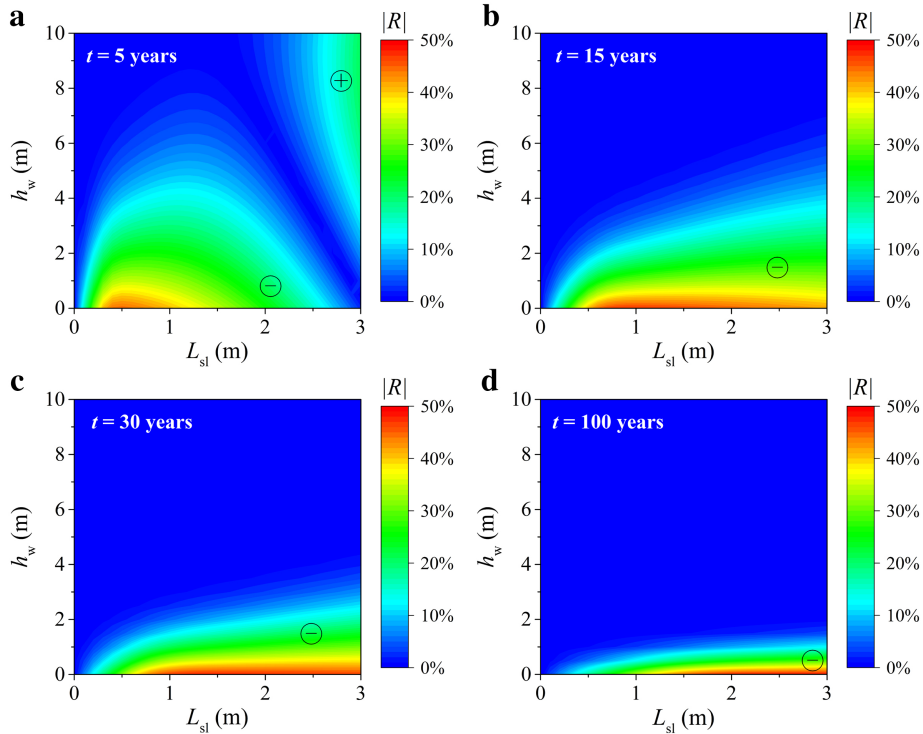


Figure 8

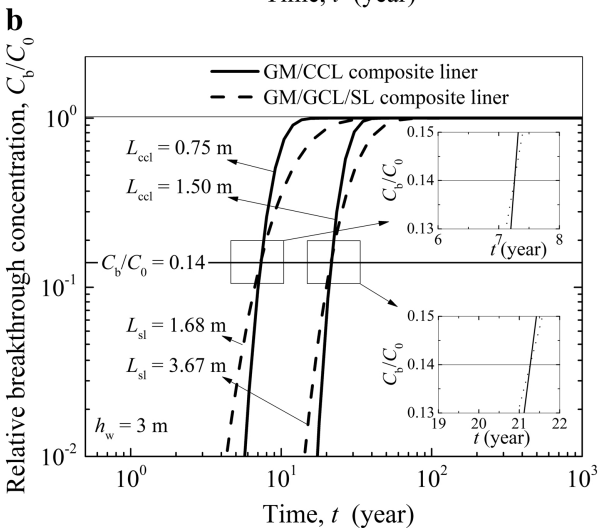
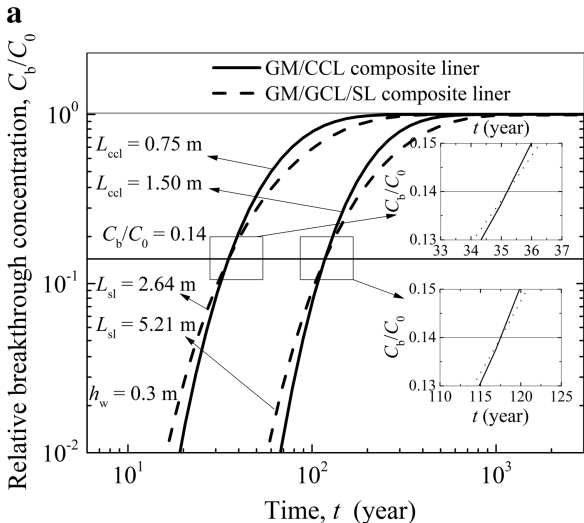


Figure 9

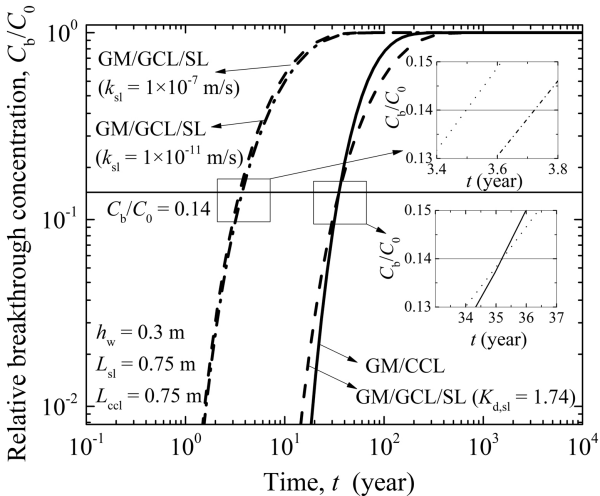


Figure 10